

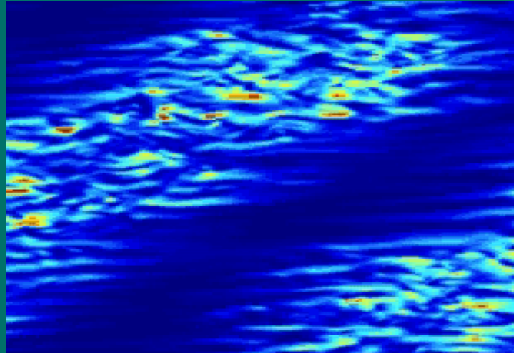
Extremes in Chaotic Dynamical Systems

Valerio Lucarini

valerio.lucarini@zmaw.de

D. Faranda, T. Kuna, P. Manneville,
G. Turchetti, S. Vaienti, J. Wouters

September 26th 2013, Budapest



1. Introduction
2. Classical Theory: Extreme Values for i.i.d. Variables
3. Extreme Values in Dynamical Systems: Theoretical Background
4. Numerical Algorithms for studying Extremes
5. Beyond Extreme Values Statistics: a New Indicator of Stability
6. Physical Observables
7. Response Theory
8. Results on the Plane Couette flow
9. Simple stochastic models
10. Final Remarks

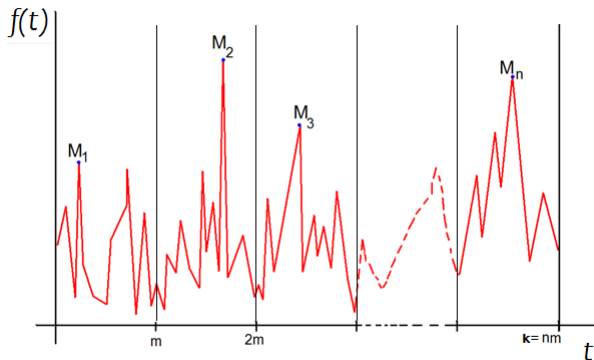
Motivations

Why are extremes important for understanding basic features of dynamical systems?

- **We have been learning** of relevance of extremes for **theory and applications**
- **Some theorems** ensure that **extremes of special observables in mixing Dynamical Systems are GEV-distributed.**
- **Extremes** can provide **information on rather refined properties of the invariant measure.**
- **Is it possible to introduce** numerical models and algorithms allowing for testing rigorously the previous properties **when finite data sets are considered?**
- **We wish to present** new results that suggest the possibility of developing **a theory of extremes for general observables** when Axiom A systems are considered.
- **We can also show that** it is possible to draft a response theory for computing **the sensitivity of the extremes to perturbations**

What is an Extreme Value? (1/3)

The Block Maxima approach



From the $f(t)$ series we select a total of n maxima M_n .
Each maximum is taken every m observations

What is an Extreme Value? (2/3)

The Generalized Extreme Value (GEV) distribution

For independent and identically distributed variables (i.i.d.), **Gnedenko** stated conditions on the parent distribution of $f(t)$ such that **the cumulative distribution of maxima M_n converges, asymptotically, to the GEV distribution:**

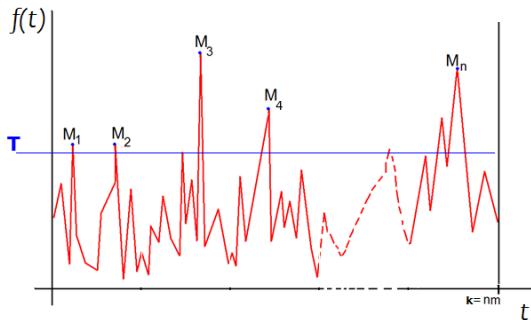
$$F_G(x; \mu, \sigma, \xi) = \exp \left\{ - \left[1 + \xi \left(\frac{x - \mu}{\sigma} \right) \right]^{-1/\xi} \right\}$$

which holds for $1 + \xi(x - \mu)/\sigma > 0$.

- μ is the **location parameter**: fit for bins of length m is $1/a_m$
- σ is the **scale parameter**: fit for bins of length m is b_m
- ξ discriminates the **type of distribution**:
 - $\xi \rightarrow 0$: Type 1 (Gumbel distribution)
 - $\xi > 0$: Type 2 (Frechet distribution)
 - $\xi < 0$: Type 3 (Weibull distribution).

What is an Extreme Value? (3/3)

The Peak over threshold approach



We set a threshold T on the $f(t)$ series.

We take all the M_n above the threshold. We shall see later.

We start by looking at the GEV approach.

Extremes in Dynamical Systems:

What do we need to observe Extreme Value Distributions in Dynamical Systems?

We will consider discrete time dynamical systems $x_{t+1} = h(x_t)$

- **Nicolis, Balakrishnan et al.** have shown no convergence to GEV distribution in regular dynamical systems.
- **Vannitsem, Felici et al.** have shown that in practical cases the convergence to GEV distribution depends strongly on the chosen observable (in particular: grid point statistics are mmmmmhhhhh)
- **Freitas, Todd and Collet et al.** have shown that for mixing systems the convergence is achieved if a particular class of observables is chosen.

In order to obtain asymptotic convergence to the GEV distribution for extremes in dynamical systems we need:

- To prove some **short- and long-term mixing conditions** - D , D' , $D2$.
- To choose suitable **observable functions**.

In order to infer the GEV parameters from the outputs of dynamical systems we need:

- .. patience.
- to be able to control the rate of asymptotic convergence.

Extremes in Dynamical Systems

Hitting Time Statistics: clarifying the role of the dynamics

Instead of proving **mixing conditions** we can check the properties on the **Hitting Time Statistics** around the point ζ :

- Exponential HTS \longleftrightarrow EVT

The recurrence time τ_A in a measurable set $A \in \Omega$, as

$$\tau_A(x) = \inf_{t \geq 1} \{x \in A : f^t(x) \in A\},$$

and the average recurrence time $\langle \tau_A \rangle$ as

$$\langle \tau_A \rangle = \int \tau_A(x) d\mu_A(x) \quad \mu_A(B) = \frac{\mu(A \cap B)}{\mu(A)},$$

We define the Hitting Time Statistics as the following limit (whenever it exists):

$$H(t) = \lim_{\mu(A) \rightarrow 0} \mu_A(A_{>t}) \quad A_{>t} \equiv \left\{ x \in A : \frac{\tau_A(x)}{\langle \tau_A \rangle} > t \right\}. \quad (1)$$

Extremes in Dynamical Systems:

The choice of the observable functions (1/2)

According to Freitas et al. (2009, 2011), following Collet (2001) found that we have an exponential HTS on balls around almost any point ζ on the attractor if and only if extreme value laws apply for the observables of type

$$g_i(\text{dist}(x, \zeta)),$$

$i = 1, 2, 3$ described in the next slide.

Axiom A systems obey these properties.

Among the invariant measures we will choose the physical one.

- The observable function $g_i(\text{dist}(x, \zeta))$ **must achieve a global maximum at $x = \zeta$ and be monotonically decreasing.**
- With the Block Maxima approach procedure, asymptotically we get a GEV distribution whose parameters **depend on the local dimension $D(\zeta)$ of a ball centered on ζ .**

Extremes in Dynamical Systems:

The choice of the observable functions (2/2)

The behavior of the tail of the distribution discriminates the type of GEV we get. It has been proven that:

- ① $\mathbf{g}_1(\mathbf{dist}(\mathbf{x}, \zeta)) = -\log(\mathbf{dist}(\mathbf{x}, \zeta)) \rightarrow$ **type 1** dist.

$$\text{At first order: } \xi = 0, \quad \sigma = \frac{1}{D(\zeta)}, \quad \mu = \frac{\log(m)}{D(\zeta)}$$

- ② $\mathbf{g}_2(\mathbf{dist}(\mathbf{x}, \zeta)) = (\mathbf{dist}(\mathbf{x}, \zeta))^{-1/\alpha} \rightarrow$ **type 2** dist. The parameter $\alpha > 0, \alpha \in \mathbb{R}$

$$\text{At the first order: } \xi = \frac{1}{\alpha D(\zeta)}, \quad \sigma = m^{\frac{1}{\alpha D(\zeta)}}, \quad \mu = m^{\frac{1}{\alpha D(\zeta)}}$$

- ③ $\mathbf{g}_3(\mathbf{dist}(\mathbf{x}, \zeta)) = \mathbf{C} - (\mathbf{dist}(\mathbf{x}, \zeta))^{1/\alpha} \rightarrow$ **type 3** dist. The constant $\mathbf{C} \in \mathbb{R}$.

$$\text{At first order: } \xi = -\frac{1}{\alpha D(\zeta)}, \quad \sigma = m^{\frac{-1}{\alpha D(\zeta)}}, \quad \mu = \mathbf{C}.$$

Extremes in Dynamical Systems:

A sort of central limit theorem

The convergence is ensured only asymptotically and two limits must be ideally satisfied:

- 1 **The number of observations m** in each bin should be extremely large
- 2 **The number of maxima n** should provide a wide enough statistics.

We first investigated the applicability of the theory on low dimensional maps:

What is the order of n and m we need to apply the theory?

Fixed series length
 $k = m \cdot n = 10^7$ iterations of the map.

- **We compute the series of the observables** and then divide them into n bins each containing m iterations.
- Varying n (and consequently m) **we check the experimental distribution parameters against the theoretical ones.**
- The following results are for the f_1 observable but the other observables behave in the same way.
- **Different mixing low-dimensional maps have been used,** (Bernoulli Shift, Arnold Cat Map, Logistic Map, IFS, Henon, Lozi, Baker).

The Logistic Map:

$$x_{t+1} = 4x_t(1 - x_t)$$

has an absolutely continuous invariant measure (a.c.i.m.).

- It is a **one dimensional, mixing map**, so we expect to find $D(\zeta) = 1$ for almost all the points $\zeta \in [0, 1]$
- The results are shown for the observable f_1 , for which we expect to find:

$$\xi = 0 \quad \sigma = 1$$

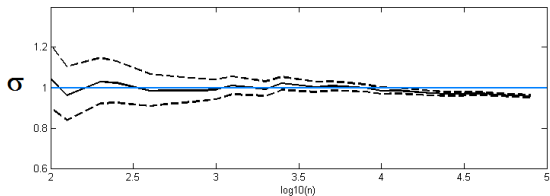
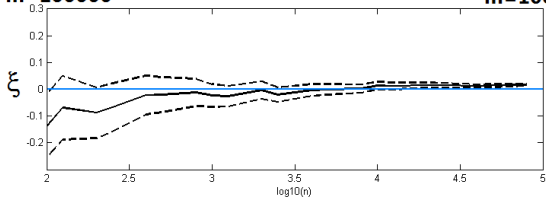
Numerical Algorithms for studying Extremes:

The dilemma of EVT inference

long bins & few true extremes

short bins & many soft extremes

$n=100$ $m=100000$ ← k fixed → $n=100000$ $m=100$



Numerical Algorithms for studying Extremes

Results on singular continuous measures

- The cdf of extremes may not absolutely continuous anymore as an effect of the inaccessible distances.
- The **GEV model gives the best continuous approximation.**
- The dimension $D(\zeta)$ implied in the GEV parameters scaling is now the **local dimension.**
- We are able to estimate with high precision the fractal dimension of e.g. the Henon, Lozi attractor
- A possible alternative to the Grassberger-Procaccia algorithm

$\Delta = 1/(\alpha \kappa)$	Baker	Hénon	Lozi
Theor.	1.4357	1.2582	1.4042
$\mu(g_2)$	1.47 ± 0.02	1.238 ± 0.009	1.396 ± 0.008
$\sigma(g_2)$	1.39 ± 0.04	1.35 ± 0.07	1.38 ± 0.02

Numerical Algorithms for studying Extremes

Example: Cantor Set (1/2)

The Cantor Set can be obtained via the following Iterating Function Systems (IFS):

$$x(1)_{t+1} = \frac{1}{3}x_t \quad x(2)_{t+1} = \frac{2}{3} + \frac{1}{3}x_t$$

where at each time step we iterate $x(1)$ or $x(2)$ with equal probability

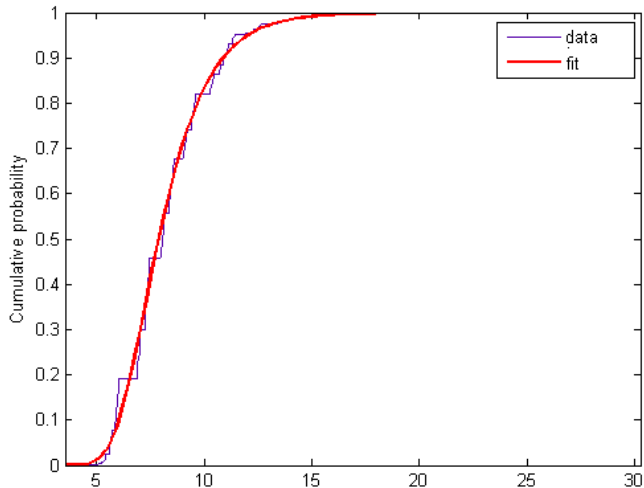
The Block maxima approach has been checked against the following theoretical results:

$$\mu \sim \log(m)/D(\zeta) \quad \sigma = 1/D(\zeta) \quad \xi = 0$$

where $D(\zeta) = \log(2)/\log(3) = 0.6309$ for almost every points belonging to the attracting set.

Numerical Algorithms for studying Extremes

Example: Cantor Set (2/2)



Numerical Algorithms for studying Extremes:

Periodic or Quasi-periodic orbits (1/2)

If in a neighborhood of a point ζ the **mixing conditions are not satisfied**, we are unable to observe a GEV distribution.

At a finite sample size, the behavior could be explained using the results of Balakrishan, Nicolis *et al.*:

Choosing as observable $f_*(t) = \min(\text{dist}(x_t, \zeta))$ and selecting the extremes with the block maxima approach we get a piecewise linear cdf

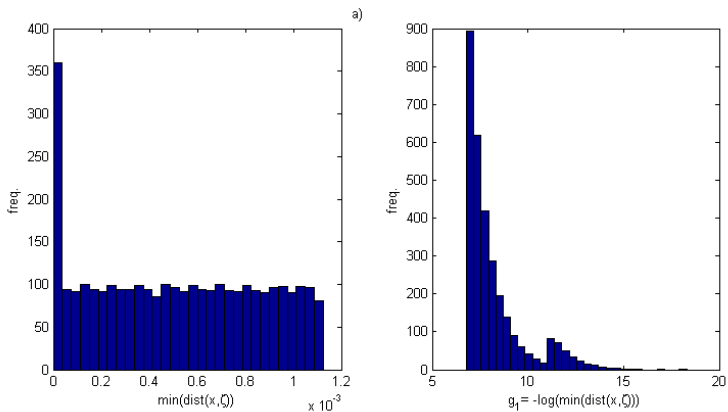
Example:

$$y_{t+1} = y_t + \frac{\kappa}{2\pi} \sin 2\pi x_t \quad x_{t+1} = y_t + x_t \pmod{1} \quad (2)$$

Standard Map: quasi periodic orbits if $\kappa \ll 1$. We set $\kappa = 10^{-4}$

Numerical Algorithms for studying Extremes:

Periodic or Quasi-periodic orbits (2/2)



Mixing Orbits:

- **Maxima** of selected observable (f_i family) **are asymptotically distributed according to the GEV distribution.**
- The theory works both for absolute continuous and singular continuous invariant measures.

Quasi-periodic Orbits:

- Minima of selected observable (f_* family) have a piecewise linear cdf.
- **Maxima** of f_i family observables **do not converge to a GEV distribution.**

Beyond the Extremes' statistics: a new Indicator of Stability

The idea: Using extremes to discriminate chaotic and regular orbits

$$A \Rightarrow B \Leftrightarrow \neg B \Rightarrow \neg A$$

Since we observe convergence to GEV distribution only if the orbit satisfies mixing requirements, we can try to use extremes to discriminate chaotic and regular behaviors.

EXAMPLE

The Standard map has a **coexistence of chaotic & regular orbits**.

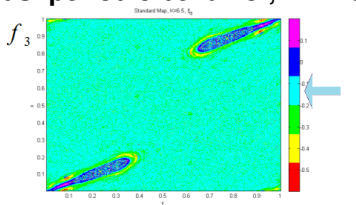
Taking different initial conditions on the 2-d torus we compute the extreme value statistics parameter and check it against the expected theoretical values. We have a convincing way to detect the *regular islands*.

Beyond the Extremes' statistics: a new Indicator of Stability

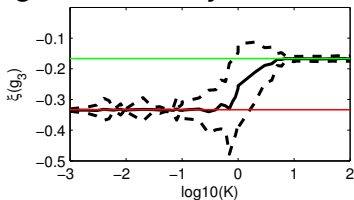
An experiment on the Standard map

Estimates of $D(\zeta)$ through the parameter ξ

In the blue regions quasi-periodic behavior, EVT is not observed

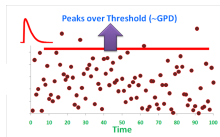


Ensemble averages: uncertainty is low for high & low K

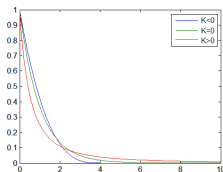
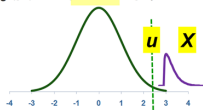


Three steps

- Only events above a given threshold are selected: we select the tail of the distribution
- We want to estimate the probability of events smaller than a certain value, given that they are larger than the threshold
- Like for the GEV, the shape parameter give the qualitative properties of the resulting distribution



$$F_U(y) = P(X - u \leq y \mid X > u)$$



GPD and GEV are step brothers

R. Deidda: Valerio, why using GEV, are you a fool? GPD works way better!

Extremes should be extremes

- Cumulative Generalised Pareto Distribution
- Asymptotic link between GEV and GPD
- Fact: shape parameters are the same
- GPD methods used to fit GEV

$$F_{GPD}(z; \xi, \sigma) = \begin{cases} 1 - \left(1 + \frac{\xi z}{\sigma}\right)^{-1/\xi} & \text{for } \xi \neq 0, \\ 1 - \exp\left(-\frac{z}{\sigma}\right) & \text{for } \xi = 0, \end{cases} \quad (3)$$

where the range of z is $0 \leq z < \infty$ if $\xi \geq 0$ and $0 \leq z \leq -\sigma/\xi$ if $\xi < 0$.

The relation between GEV and GPD parameters has been already discussed in literature in case of i.i.d variables [7–10]. It is first interesting to note that

$$F_{GPD}(z - T; \sigma, \xi) = 1 + \log(F_{GEV}(z; T, \sigma, \xi)) \quad (4)$$

for $F_{GEV}(z; \mu, \alpha, \kappa) \geq \exp^{-1}$, where the latter condition implies $z \geq T$ [11]. If we consider the upper range $z \gg T$, we have that $F_{GEV}(z; T, \sigma, \xi)$ is only slightly smaller than 1, so that Eq. 4 implies that

$$F_{GPD}(z - T; \sigma, \xi) \sim F_{GEV}(z; T, \sigma, \xi) + O\left(\left(1 + \xi(z - T)/\sigma\right)^{-2/\xi}\right),$$

GPD overcomes the difficulties of GEV

- A threshold T is a radius $r^* \rightarrow$

- Conditional probability \rightarrow

- Complementary cumulative function

- We are close!

We study the exceedance above a threshold T defined as $T = g(r^*)$. We obtain an exceedance every time the distance between the orbit of the dynamical system and ζ is smaller than r^* . Therefore, we define the exceedances $z = g(r) - T$. By the Bayes' theorem, we have that $P(r < g^{-1}(z + T) | r < g^{-1}(T)) = P(r < g^{-1}(z + T)) / P(r < g^{-1}(T))$. In terms of invariant measure of the system, we have that the probability $H_{g,T}(z)$ of observing an exceedance of at least z given that an exceedance occurs is given by:

$$H_{g,T}(z) \equiv \frac{\nu(B_{g^{-1}(z+T)}(\zeta))}{\nu(B_{g^{-1}(T)}(\zeta))}. \quad (12)$$

Obviously, the value of the previous expression is 1 if $z = 0$. In agreement with the conditions given on g , the expression contained in Eq. (12) monotonically decreases with z and vanishes when the radius is given by $g^{-1}(g_{max})$. Note that the corresponding cdf is given by $F_{g,T}(z) = 1 - H_{g,T}(z)$.

GPD approach is just a magnifying glass

... with a suitable weighting

- We assume a local scaling of the measure of the attractor:

$$\lim_{r \rightarrow 0} \frac{\log \nu(B_r(\zeta))}{\log r} = D(\zeta), \text{ for } \zeta \text{ chosen } \nu - \text{a.e.}$$

- We translate this mass scaling into the equation for $H_{g,T}$:

$$H_{g,T}(z) \sim \left(\frac{g^{-1}(z+T)}{g^{-1}(T)} \right)^D$$

- This is a VERY general result
- Axiom A: $D(\zeta) = D = d_H \simeq d_{KY}$
- mixing dynamics: local \rightarrow global

Let's specify the results for the g'_i s observables

Functional form of the g'_i s:

$$g_1(r) = -\log(r)$$

$$g_2(r) = r^{-\beta}$$

$$g_3(r) = C - r^\beta$$

- g_1 -type observable:

$$\sigma = \frac{1}{D} \quad \xi = 0;$$

- g_2 -type observable:

$$\sigma = \frac{T\beta}{D} \quad \xi = \frac{\beta}{D};$$

- g_3 -type observable:

$$\sigma = \frac{(C - T)\beta}{D} \quad \xi = -\frac{\beta}{D}.$$

We lost track of them!

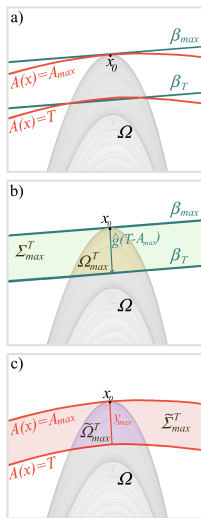
- GPD: where are the conditions on the dynamics?
- Example: in a quasi-periodic system, choosing VERY long blocks, with GEV approach you end up choosing more or less always the same maximum
- With GPD, the observable acts as a magnifying glass near $\zeta \rightarrow$ info on the local geometrical properties
- With mixing, (e.g. Axiom A), we get global information
- **Pareto \rightarrow geometry, Gnedenko \rightarrow dynamics**
- **They give the same information when geometry and dynamics *commute* \rightarrow mixing conditions**

Distance observables are not very *physical*

- unless one looks at recurrences of the orbits \rightarrow *weather analogues*
- Example: we want to look at *energy-like* observables of the form $\langle \vec{x}, M\vec{x} \rangle$ where \vec{x} is a point in the phase space, M is a matrix, and $\langle \bullet, \bullet \rangle$ is the scalar product
- In Fluid Dynamics, many physical observables can be written in this form!
- More in general, we want to study the extremes of $A : \vec{x} \in \mathbb{R}^n \rightarrow A(\vec{x}) \in \mathbb{R}$.
- Difference *wrt* previous case: **Geometry of the portion of attractor where extremes are realized**

Construction

- $A(x)$ has isolated max A_{max} in $x_0 \in \Omega$
- β_{max} is tangent to $A(x) = A_{max}$ in x_0
- \hat{g} is parallel to $\nabla A(x)|_{x=x_0} \neq 0$
- $A(x) = T$ is threshold, β_T is $\beta_{max} \rightarrow \hat{g}$
- Extremes of $A(x)$ are in $\tilde{\Omega}_{max}^T \dots$
- ... as $T \rightarrow A_{max}$, $\tilde{\Omega}_{max}^T \sim \Omega_{max}^T$



Indeed not a the intersection of a ball with a fractal set!

- Exceedance $A(x) - T$ is \propto distance btw x and β_T
- Complementary cumulative function comes from conditional probability

We define the exceedances for the points $x \in \tilde{\Omega}_{A_{max}}^T$ as $z = A(x) - T$. An exceedance z corresponds geometrically to a distance $y = \text{dist}(x, \beta_T) = z/|\nabla A|_{x=x_0}|$ from β_T and a distance $k = \text{dist}(x, \beta_{max}) = y_{max} - y = (A_{max} - T)/|\nabla A|_{x=x_0}| - z/|\nabla A|_{x=x_0}|$ from β_{max} .

Therefore, $P(z > Z | z > 0) = P(y > Y | y > 0)$, where $Y = Z/|\nabla A|_{x=x_0}|$. We have that $P(y > Y | y > 0) = P(y > Y)/P(y > 0)$. In terms of the invariant measure of the system, we have that the probability $H_T(Z)$ of observing an exceedance of at least Z given that an exceedance occurs is given by:

$$H_T(Z) \equiv \frac{\nu(\Omega_{A_{max}}^{T+Z})}{\nu(\Omega_{A_{max}}^T)}. \quad (5)$$

where we have used the ergodicity of the system. Obviously, the value of the previous expression is 1 if $Z = 0$. The expression contained in Eq. (5) monotonically decreases with Z (as $\Omega_{A_{max}}^{T+Z_2} \subset \Omega_{A_{max}}^{T+Z_1}$ if $Z_1 < Z_2$) and vanishes when $Z = A_{max} - T$.

General Result

- We assume the flow is Axiom A so to relate local and global measures of the dimension of the attractor
- Assuming generic geometry (!) ... $\nu \left(\Omega_{max}^{T+Z} \right) \propto (A_{max} - T - Z)^\delta$
- where $\delta = d_s + d_u/2 + d_n/2$ regardless of the observable
- $d_s/d_u/d_n (= 1)$ are the stable/unstable/neutral direction of the flow
- Final result (See also: Holland et al. 2011, GEV approach):

$$H_T(Z) \approx \frac{(A_{max} - T - Z)^\delta}{(A_{max} - T)^\delta} = \left(1 - \frac{Z}{A_{max} - T} \right)^\delta. \quad (8)$$

Note that the corresponding cdf is given by $F_T(Z) = 1 - H_T(Z)$. Comparing Eqs. 3 and Eqs. 8, one obtains that $F_T(Z)$ belongs to the GPD family, and that the GPD parameters can be expressed as follows:

$$\xi = -1/\delta \quad (9)$$

$$\sigma = (A_{max} - T) \cdot / \delta. \quad (10)$$

Extremes → Partial Dimensions

- We have $\xi_A = -1/\delta = -1/(d_s + d_n/2 + d_u/2)$: ξ_A is negative because the attractor is **compact**
- ... But, in practical applications, the system can take long time to realize this!
- Let's take $B(x) = -\text{dist}(x, x_0)^\beta$, $\beta > 0$.
- We have: $\xi_B = -\beta/d_{KY} = -\beta/(d_s + d_n + d_u)$
- We derive:

$$\frac{2}{\xi_A} - \frac{2\beta}{\xi_B} = d_u + d_n$$
$$\frac{\beta}{\xi_B} - \frac{2}{\xi_A} = d_s$$

- Partial dimensions along the stable and unstable directions & extremes related to $x = x_0$.

Shape Parameter from Empirical Moments

GPD density:

$$f_{GPD}(z; \xi_A, \sigma_A) = \frac{d}{dz} (F_{GPD}(z; \xi_A, \sigma_A))$$

First two moments:

$$\int_0^{-\sigma_A/\xi_A} dz z f_{GPD}(z; \xi_A, \sigma_A) = \frac{\sigma_A}{1 - \xi_A} = \mu_1$$
$$\int_0^{-\sigma_A/\xi_A} dz z^2 f_{GPD}(z; \xi_A, \sigma_A) = \frac{2\sigma_A^2}{(1 - \xi_A)(1 - 2\xi_A)} = \mu_2.$$

It is easy to derive that

$$\xi_A = \frac{1}{2} \left(1 - \frac{\mu_1^2}{\mu_2 - \mu_1^2} \right) = \frac{1}{2} \left(1 - \frac{1}{id_A} \right).$$

id_A is the index of dispersion

Shape Parameter from Observables

Rewriting the moments in terms of conditional invariant measure:

$$\mu_1^T = \frac{\int \rho_\epsilon(dx) \Theta(A(x) - T)(A(x) - T)}{\int \rho(dx) \Theta(A(x) - T)} = \frac{\langle \tilde{A}_1 \rangle^T}{\langle \tilde{A}_0 \rangle^T}$$
$$\mu_2^T = \frac{\int \rho(dx) \Theta(A(x) - T)(A(x) - T)^2}{\int \rho(dx) \Theta(A(x) - T)} = \frac{\langle \tilde{A}_2 \rangle^T}{\langle \tilde{A}_0 \rangle^T}.$$

Expression for the shape parameter:

$$\xi_A^T = \frac{1}{2} \left(1 - \frac{(\langle \tilde{A}_1 \rangle^T)^2}{\langle \tilde{A}_2 \rangle^T \langle \tilde{A}_0 \rangle^T - (\langle \tilde{A}_1 \rangle^T)^2} \right),$$

where the result is exact in the limit for $T \rightarrow A_{max}$:

$$\xi_A = \lim_{T \rightarrow A_{max}} \xi_A^T.$$

Same applies for B observables.

A Response Theory for Extremes (1/3)

A brief recap of Ruelle's response theory for Axiom A systems:

- We perturb $\dot{x} = G(x) \rightarrow \dot{x} = G(x) + \epsilon X(x)$, where ϵ is small
- Evolution operator $f^t \rightarrow f_\epsilon^t$ and the invariant measure $\rho_0 \rightarrow \rho_\epsilon$.
- We can write $\langle \Psi \rangle_\epsilon = \langle \Psi \rangle_0 + \sum_{j=1}^{\infty} \epsilon^j \langle \Psi^{(j)} \rangle_0$
- $\langle \Psi^{(j)} \rangle_0$ time-integral of a Green function
- Useful formula:
$$\left. \frac{d^n \langle \Psi \rangle_\epsilon}{d\epsilon^n} \right|_{\epsilon=0} = n! \langle \Psi^{(n)} \rangle_0.$$
- Consider $n = 1$ case.

A Response Theory for Extremes (2/3)

- Even if Θ is not smooth, we can derive for every $T < A_{max}$:

$$\left. \frac{d\xi_A^{T,\epsilon}}{d\epsilon} \right|_{\epsilon=0} = -\frac{1}{2} \frac{d}{d\epsilon} \left\{ \frac{(\langle \tilde{A}_1 \rangle^{T,\epsilon})^2}{\langle \tilde{A}_2 \rangle^{T,\epsilon} \langle \tilde{A}_0 \rangle^{T,\epsilon} - (\langle \tilde{A}_1 \rangle^{T,\epsilon})^2} \right\} \Big|_{\epsilon=0}.$$

- Recipe for sensitivity of $\xi_A^{T,\epsilon}$ at $\epsilon = 0$ for any practical case
- Formal problems emerge for existence of:

$$\lim_{T \rightarrow A_{max}} \left. \frac{d\xi_A^{T,\epsilon}}{d\epsilon} \right|_{\epsilon=0} = \lim_{T \rightarrow A_{max}} \lim_{\epsilon \rightarrow 0} \frac{\xi_A^{T,\epsilon} - \xi_A^{T,0}}{\epsilon}$$

- Not clear whether such limit is equal to $\lim_{\epsilon \rightarrow 0} \lim_{T \rightarrow A_{max}} \frac{\xi_A^{T,\epsilon} - \xi_A^{T,0}}{\epsilon}$
- If limits exist and equal \rightarrow response theory for ξ_A (same for ξ_B).

Extremely bizarre results follow from this

- Assume: ξ_A & ξ_B diff. & system struct. stable (strong trans.)
- Remember: ξ_A and ξ_B can be expressed in terms of d_s , d_n , d_u .

$$\left. \frac{d\xi_A^\epsilon}{d\epsilon} \right|_{\epsilon=0} = \left\{ \frac{1}{(d_s^\epsilon + d_u^\epsilon/2 + d_n^\epsilon/2)^2} \frac{d(d_{KY}^\epsilon)}{d\epsilon} \right\} \Big|_{\epsilon=0}.$$

$$\left. \frac{d\xi_B^\epsilon}{d\epsilon} \right|_{\epsilon=0} = \left\{ \frac{\beta}{d_{KY}^{\epsilon^2}} \frac{d(d_{KY}^\epsilon)}{d\epsilon} \right\} \Big|_{\epsilon=0};$$

- Derivative of d_{KY}

$$\begin{aligned} \left. \frac{d(d_{KY}^\epsilon)}{d\epsilon} \right|_{\epsilon=0} &= - \left\{ \frac{(d_s^\epsilon + d_u^\epsilon/2 + d_n^\epsilon/2)^2}{2} \right\} \Big|_{\epsilon=0} \times \\ &\times \left\{ \frac{d}{d\epsilon} \frac{(\langle \tilde{A}_1 \rangle^{T,\epsilon})^2}{\langle \tilde{A}_2 \rangle^{T,\epsilon} \langle \tilde{A}_0 \rangle^{T,\epsilon} - (\langle \tilde{A}_1 \rangle^{T,\epsilon})^2} \right\} \Big|_{\epsilon=0} \end{aligned}$$

If one of ξ_A , ξ_B or d_{KY} differentiable, all are differentiable

If ξ_A increases with $\epsilon \rightarrow \xi_A$ closer to zero

- ϵ -perturbation increases the Kaplan-Yorke dimension
- ϵ -perturbation increases the index of dispersion
- Qualitatively, it favors *forcing over dissipation* \rightarrow larger extremes

Weak statement: connection btw regularity of ξ_A , ξ_B , and d_{KY} wrt perturbations.

- Numerical experience shown that these quantities are *relatively* regular when we consider high-dimensional systems
- Not so in low dimensional systems!!!
- Same with Lyapunov exponents, etc: if this were not the case, data assimilation, models tuning, etc would be hopeless. But...

- 1 Relationship between GEV/GPD parameters and Local Dimension Attractor.
- 2 Numerical algorithms corresponding to limits in theorems.
- 3 GEV parameters as Dynamical Indicators of Stability.
- 4 GPD theory more informative of the geometry of the system, but misses dynamics.
- 5 EVT for Physical Observables in Axiom A systems.
- 6 From Extremes to Partial Dimensions in Stable/Neutral/Unstable Directions.
- 7 Establishment of Response Theory.
- 8 Differentiability of Shape Parameter/Differentiability of d_{KY} .

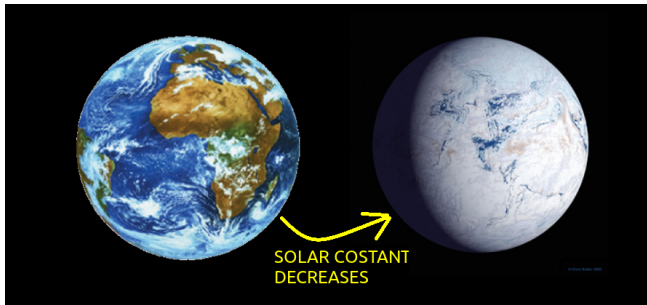
Selected References

- Faranda, D., Lucarini, V., Turchetti, G. & Vaienti, S. [2011] Numerical convergence of the block-maxima approach to the Generalized Extreme Value distribution, J. Stat. Phys. 145, 1156
- Faranda, D., Lucarini V, Turchetti, G. & Vaienti, S. [2011] Generalized Extreme Value distribution parameters and dynamical indicator of stability, Int. Jou. Bif. Chaos 22, 1250276
- Lucarini, V., Faranda, D., Turchetti, G. & Vaienti, S. [2012] Extreme Value distribution for singular measures, Chaos 22, 023135
- Lucarini, V., Faranda, D., & Wouters, J. [2012] Universal behavior of extreme value statistics for selected observables of dynamical systems, J. Stat. Phys. 147, 63
- Lucarini, V., Kuna, T, Faranda, D., & Wouters, J. [2012] Towards a General Theory of Extremes for Observables of Chaotic Dynamical Systems, arXiv:1301.0733 [cond-mat.stat-mech]

Studying critical transitions

What is a critical transition in Earth sciences?

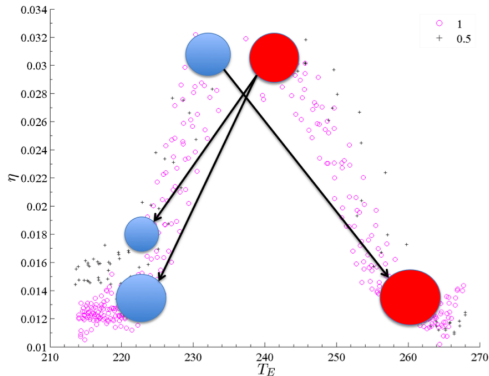
A popular example: The day after tomorrow



- **Critical transition:** abrupt change of the properties of a system.
- Corresponds to a **bifurcation**, which results into a change of the **physical measure** (supported in the attractor).
- Three main classes of bifurcations: **parametrically induced**, rate-induced, and **noise-induced**.

What is a critical transition in Earth sciences?

The Snowball Earth example.



- Efficiency of the climate engine: $\eta = \frac{\Phi^h - \Phi^c}{\Phi^h} = \frac{T_W - T_C}{T_W}$
- At critical transitions η decreases \rightarrow system closer to equilibrium \rightarrow system more stable \checkmark (Boschi et al. 2013, Icarus).

What about detecting tipping points? Traditional approach

Mainstream approaches - see e.g. **Scheffer et al. (2009)**:

- **Critical slowing down**: as the system approaches such critical points, it becomes increasingly slow in recovering from small perturbations.
- The slowing down should lead to **an increase in autocorrelation** in the resulting pattern of fluctuations.
- **Increased variance in the pattern of fluctuations** is another possible consequence of critical slowing down: the effect of perturbations accumulates.
- As made clear by Ditlevsen: if we want to use the usual simple model of tipping point to interpret data, all of these properties must be observed near a critical transition

- **These indicators are so and so when a Hopf bifurcation is approached:** slowing down & long transient oscillations.
- Departure from Gaussianity not useful if even far from bifurcation the time series is not Gaussian, and already in few d.o.f. systems, the two-well model may lead to major mistakes in the time scales
- **Internal fluctuations** (which bring the system to the border of a basin of attraction) **are not associated with particular properties of specific stable or unstable points**
- **Spatially extended and/or high dimensional systems may have very complicated bifurcation patterns**
- *Freidlin-Wentzell theory may allow for studying rigorously tipping points, we are not quite there.*

The advantages of using Extreme Value Theory

- The indicators used by **Scheffer** cover statistical properties which are related **only to the first moments of the data distribution**.
- This lacks universality; we want to look for more intrinsic characterizations of large fluctuations.
- ... well, this is exactly what Extreme Value Theory does!
- Recently, rigorous extreme value laws have been established for chaotic dynamical systems for various classes of observables.

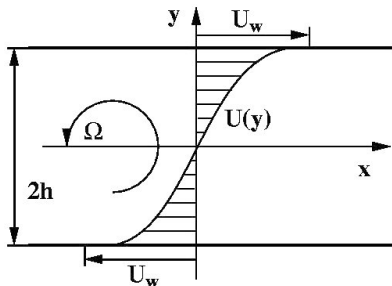
GOAL

Find sensitivities of extremes when nearing tipping points
Study the boundary between the basins of attraction

The Plane Couette Flow

The Plane Couette Flow

- This flow is ideally obtained by **shearing a fluid between two infinite parallel plates** at a distance $2h$ moving in opposite directions at speeds U_w , which defines the stream-wise direction x , y and z being the wall-normal and span-wise directions, respectively.
- The **laminar profile** is just $U_b(y) = U_w = y/h$
- The **Reynolds number** is $Re = U_w h / \nu$.



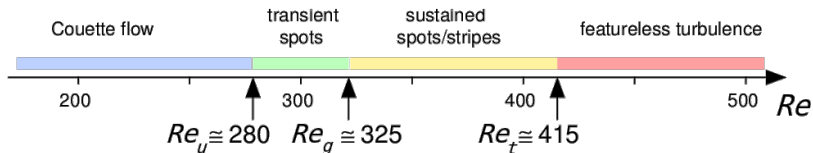
Motivations

Transitions in the Plane Couette flow

- The linear velocity profile is linearly stable at all values of Re : no gradient of background vorticity.
- In fact, the laminar flow is observed only for a limited range of $Re < Re_U$, It is known that for larger values of Re , the size of the basin of attraction to the laminar state is extremely small but non-vanishing.
- Whenever we observe in practice a persistent turbulent state, we in fact in a regime where the system is multistable: the laminar and turbulent states cohesist
- The transition to turbulence of the plane Couette flow is an open problem of fluid dynamics

Phenomenology of the Plane Couette flow

Bifurcations

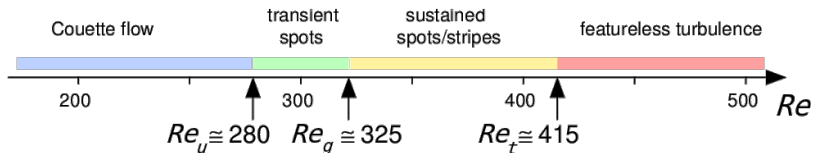


Bifurcation of the plane Couette flow as obtained by the Saclay group.

- For $Re < Re_u \simeq 280$, the **laminar profile is rapidly recovered** whatever the intensity of the perturbation brought to the flow.
- For $Re_u < Re \lesssim Re_g = 325$, **turbulence is only transient** but as Re_g is approached from below, the lifetime of turbulence increases.
- For $Re_g \lesssim Re \lesssim 360$ turbulence takes the form of **irregular large spots**.

Phenomenology of the Plane Couette flow

Bifurcations

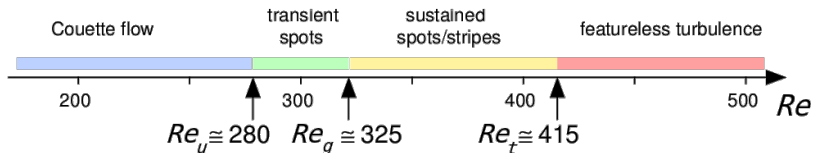


Bifurcation of the plane Couette flow as obtained by the Saclay group.

- For $360 \lesssim Re \lesssim Re_t = 415$ **the spots merge to form oblique stripes**. These stripes are characterised by a regular modulation of the turbulence intensity which dies out when Re_t is approached from below.
- For $Re_t \lesssim Re$ a regime of **featureless turbulence is observed**.

Phenomenology of the Plane Couette flow

Hysteresis and bands structure in the reverse transition



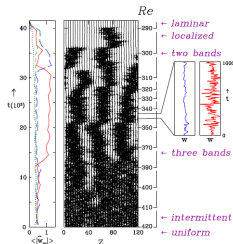
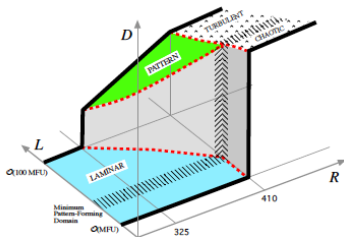
Bifurcation of the plane Couette flow as obtained by the Saclay group.

- In the **forward transition**, obtained increasing Re , the dynamics is characterized by **the presence of turbulent spots**.
- The **reverse transition** is marked by the occurrence of **oblique turbulent bands**, only observable in very large aspect ratio systems, ($Re_g < Re < Re_t$).

Phenomenology of the Plane Couette flow

More on the bifurcations

- The presence of bands structure in numerical simulations is an encouraging sign of the **robustness of the structure itself** and on the possibility of investigating numerically the problem.
- Not yet a theory explaining the transition** with the suppression of the bands



A spatiotemporal process if system is extended.

The data analyzed have been provided by numerical simulations performed by P. Manneville using the code *channelflow*.

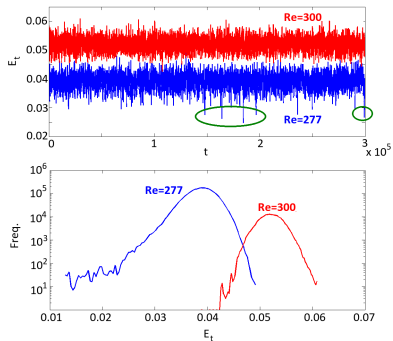
- Low: $N_y = 15$, $N_x = 108$, $N_z = 192 \rightarrow [R_g; R_t] = [275; 350]$
- Medium: $N_y = 21$, $N_x = 216$, $N_z = 384 \rightarrow [R_g; R_t] = [300; 380]$
- High: $N_y = 27$, $N_x = 324$, $N_z = 384 \rightarrow [R_g; R_t] = [325; 405]$

The typical length of the series is
 $k = m \cdot n \simeq 3 \cdot 10^5$ time units.

- **We proceed from above!**
- The observable taken is the **Perturbation Energy** E (the mean square distance to the laminar flow).
- The series of E is divided in bins. **Maxima and minima of each bin are extracted and fitted to the GEV distribution.**

The Results on Plane Couette numerical simulations (1/3)

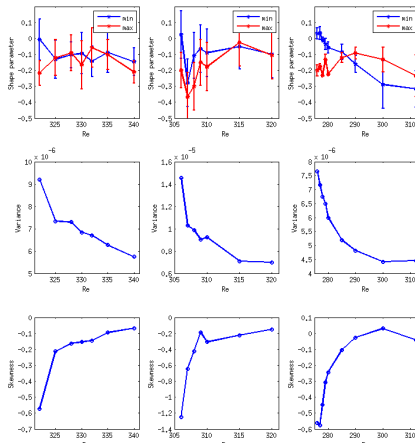
Analysis of Shape GEV parameter κ for the maxima and minima distribution VS Re



- **The shape parameter for minima distribution changes**, changing the type of GEV observed.
- **The distribution of maxima is less modified** by the changes in Reynolds number.

Results on Plane Couette numerical simulations (2/3)

Maxima and minima distribution VS $Re - Re_g$



- Consistent results for increasing resolutions!

- When The Reynolds number move towards the critical value Re_g **we observe a clear change in the sign of the shape parameter of the GEV distribution for the minima** whereas the maxima distribution belongs to the same family.
- The amplitude of fluctuations of the minima increases more than that of the maxima, as **the system "feels" the presence of the laminar state**, which rises the probability of very low levels of turbulence when Re is decreased.
- **This is instead related to the presence of the competing attracting state, which causes the increase in the skewness for the distribution of minima**

Some theoretical models for critical transitions

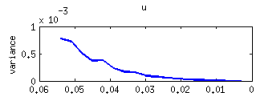
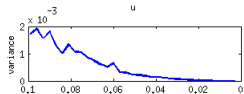
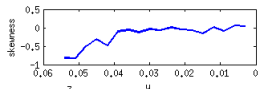
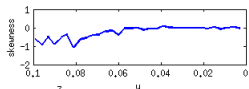
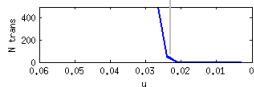
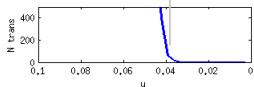
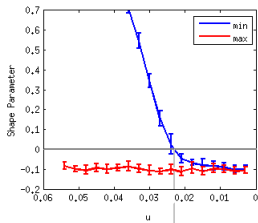
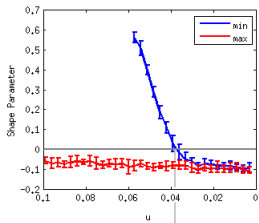
- We consider the following system of SDEs:

$$\begin{aligned}dX/dt &= -(\mu + u\xi(t))X + Y^2 \\dY/dt &= -\nu X + Y - XY\end{aligned}$$

- where $\mu, \nu \propto 1/R$ describe viscous effects and $E = 1/2X^2 + 1/2Y^2$ is conserved by the nonlinear terms, $u > 0$ and ξ is a white noise. u contributes to viscosity.
- For $\mu\nu \leq 1/4$ we have multistability, and competition between the (0,0) solution (laminar) and a turbulent state.
- We set $\mu = 1$, $\nu = 0.2475$ and $\nu = 0.2487$ and test the escape rate from the turbulent state as a function of u .
- $n = 10^3$, $m = 10^6$

Noise-induced bifurcations in Barkley's model

Transitions turbulent \rightarrow laminar



Particle in a double well potential

The experiment

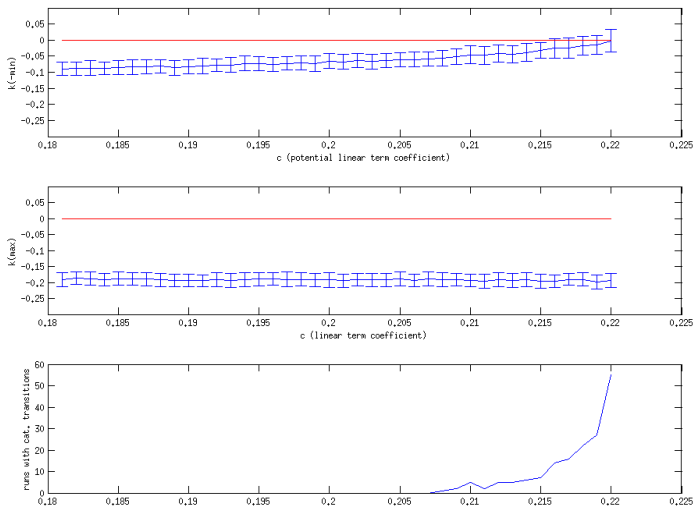
For the potential $V(x) = ax^4 + bx^2 + cx$ we keep a, b fixed while we modify c in such a way that the system is pushed towards the left well. This happens in the deterministic system when $c = c_{crit}$.

- 1 We **select an initial condition** $x_0 \sim 0.63$ and make **100 realizations** of the systems, with ϵ fixed.
- 2 For each realization we obtain a series of length $k = 10^6$ data.
- 3 We **split the series in 1000 bins each containing 1000 observations**.
- 4 For the $g_i, i = 1, 2, 3$ observables and the maxima and minima we **fit the GEV distribution** and study the behavior of the shape parameter.

If the particle falls in the left well, we interrupt the series and create another transient.

Particle in a double well potential

Analysis of Shape GEV parameter κ for the maxima and minima distribution VS c

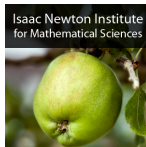


The results show the same quantitative behavior as obtained analysing the Plane Couette flow:

- Also in this case the shape parameter for **the minima distribution approach zero when we push the system through a critical transition.**
- **The shape parameter for the maxima remains more or less constant** when the potential is modified.

Final Remarks

- 1 Extremes can provide early warnings of critical transitions when the Reynolds number is decreased to $Re \sim Re_g$
- 2 Change in the minima linked to the presence of the laminar attracting state
- 3 Same quantitative results have been obtained on a simple theoretical model of critical transition
- 4 Further explore the possibility of using extremes as a generic tool to study the critical transitions
- 5 MPE 2013 Event at Newton Inst. in Cambridge, Oct-Dec 2013



Selected References

- 1 Faranda, D., Lucarini V, Turchetti, G. & Vaienti, S [2012] Generalized Extreme Value distribution parameters and dynamical indicator of stability, Int. Jou. Bif. Chaos.
- 2 Lucarini, V., Faranda, D., & Willeit, M., [2012], Bistable systems with stochastic noise: virtues and limits of effective one-dimensional Langevin equations, Nonlin. Processes Geophys., 19, 9-22
- 3 Manneville, P. and Rolland, J. [2011]: On modelling transitional turbulent flows using under-resolved direct numerical simulations: the case of plane Couette flow. Theor. Comp. Fluid Dyn 25, 407420.
- 4 Manneville, P. [2008] : Understanding the sub-critical transition to turbulence in wall flows, Pramana 70(6) 1009-1021.

Dank u voor uw aandacht!

Thank you for your attention!

Merci pour votre attention!

Vielen Dank für Ihre Aufmerksamkeit!

Grazie per la vostra attenzione!

Tack for er uppmärksamhet!

Gracias por la atención prestada!

Obrigado pela sua atenção!

Σας ευχαριστώ για την προσοχή σας!